Geostatistical Analysis of CPT-UVIF Data for Development of a Site Conceptual Model

Amir H Hosseini, PhD candidate, Department of Civil and Environmental Engineering, University of Alberta, Edmonton, AB, Canada

Kevin W Biggar, Professor, Department of Civil and Environmental Engineering, University of Alberta, Edmonton, AB, Canada

Clayton V Deutsch, Professor, Department of Civil and Environmental Engineering, University of Alberta, Edmonton, AB, Canada

Carl A Mendoza, Associate Professor, Department of Earth and Atmospheric Sciences, University of Alberta, Edmonton, AB, Canada

Abstract

Cone Penetration Testing (CPT) provides detailed information about soil type and associated design parameters. Ultra Violet Induced Fluorescence Cone Penetration Testing (CPT-UVIF) has been used frequently in environmental site characterization to delineate subsurface stratification as well as lateral and vertical hydrocarbon distribution. The information collected during site investigation provides a basis for further site investigations and for evaluating the applicability of various remedial techniques. This information, however, is incomplete which translates to uncertainty in bounding the problem and increases the risk of regulatory non-compliance or excess remediation costs. To attain a better understanding of geological structure and non-aqueous phase liquid (NAPL) distribution, this uncertainty should be assessed and quantified. Using geostatistical techniques, models of uncertainty for geological structure and NAPL distribution have been developed for a hydrocarbon impacted site. In conjunction with CPT data analysis techniques, the Sequential Indicator Simulation (SIS) approach has been used to determine the site lithology and extent of contaminant source zone. The original spatial continuity is captured and trends are reproduced. Based on the models of uncertainty for geological structure and contaminant source zone and their association, a conceptual model can be developed for the site. Results of this work will ultimately provide a framework for subsequent numerical modeling of natural attenuation of petroleum hydrocarbons at the site.

Introduction

Risk and uncertainty are characteristics of the ground and never can be eliminated, but can be quantified. Even with very extensive site investigation schemes, only a small portion of ground can be fully characterized. In every geo-environmental engineering project, there are a number of important objectives for site investigations. These include nature and sequence of the subsurface strata, groundwater conditions, physical properties of subsurface strata (e.g. hydraulic conductivity), and distribution and composition of contaminants.

Cone Penetration Testing (CPT) has two main applications in the site investigation processes associated with geo-environmental applications. One is to determine sub-surface stratigraphy and identify materials present; and the other is to estimate geo-engineering parameters (Lunne, et al 1997). In geo-engineering practice, CPT has been used frequently for soil profiling and classification. There is extensive experience in relating CPT results to soil type. Experience has shown that typically the cone penetration resistance is high in sands and low in clays and the dimensionless ratio between sleeve-friction and cone resistance (friction ratio) is low in sands and high in clays. CPT data provide a repeatable index of the aggregate behavior of the in-situ soil in the immediate area of the probe. The prediction of soil type based on CPT results is usually referred to as soil behavior type (Robertson 1998). One of the most commonly used CPT soil behavior type (SBT) charts is the one suggested by Robertson et al. (1986). Figure 1(a) shows this soil behavior type classification chart.

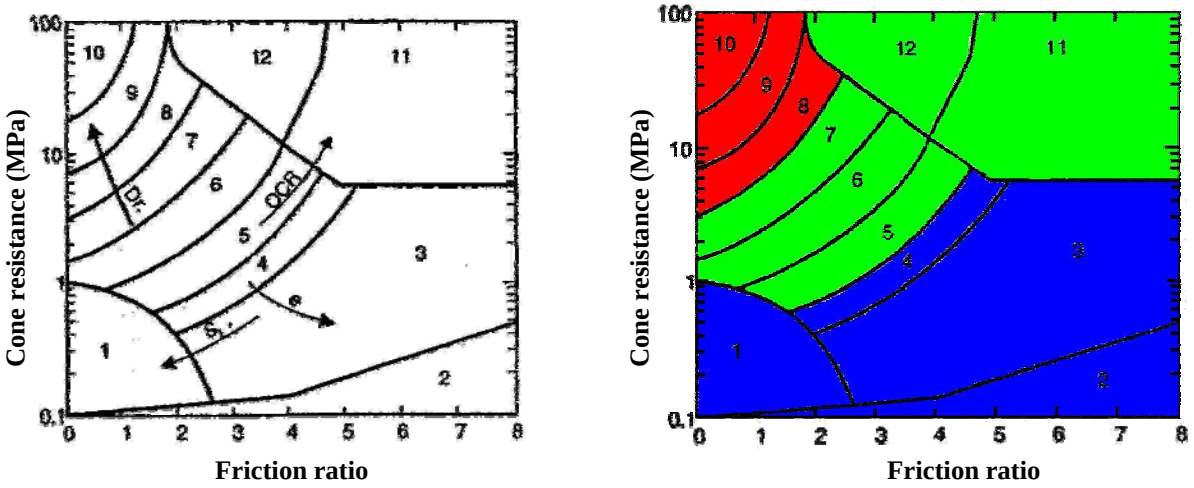

Figure 1: (left) non-normalized soil behavior type classification chart (Robertson et al. 1986) and (right) grouping SBTs into three categories based on their estimated hydraulic conductivities.

SBT classification charts may be interpreted to give an estimate of hydraulic conductivity of soils. Although these estimates are approximate, they can provide a guide to variations of hydraulic conductivity at sampling locations. To use the SBT charts in subsequent geostatistical modeling and to prevent the large-scale geological features from being masked by unrealistic short-scale variations, in this study the SBTs have been grouped into three different categories. These categories will be used as inputs for Sequential Indicator Simulation (SIS) technique to generate: (1) equi-probable realizations of geological structure for use in reproduction of hydraulic conductivity, and (2) probability maps showing continuity of geological strata at the site.

Delineation of the source zone is a very important step in environmental site characterization for sites impacted by petroleum hydrocarbons (PHCs). Non-aqueous phase liquids (NAPLs) containing aromatic hydrocarbons can be successfully detected by fluorescence. Commercially available Ultra Violet Induced Fluorescence Cone Penetrometer

(CPT-UVIF) is a standard CPT cone coupled with a module to detect ultraviolet induced fluorescence. The UVIF module consists of a high intensity UVIF light projected into the surrounding soil and a photo multiplier tube sensor to record fluorescence. The currently available CPT-based fluorescence systems are typically restricted to a single wavelength excitation source, each demonstrating specific advantages and disadvantages with respect to detection capabilities for particular fluorophores (Kram et al. 2004). According to CCME criteria, the wavelength used in this study corresponds approximately to the F4 fraction (C_{34} to C_{50}) (Canadian Council of Ministers of the Environment 2001).

In previous studies, the magnitude of fluorescence was directly related to the relative concentration of aromatic PHCs present in the soil (Armstrong, et al. 2004). Using indicator simulation techniques, in this study, a newer approach is taken by development of a model of absence/presence for NAPL contamination to remove the effects of aggregate size on UVIF recordings. This approach introduces a risk-based framework for contaminant source distribution. Continuity of hydrocarbon impacted zones is better reproduced. Effects of other controlling factors such as geological structure and stratification are also added to the model to improve the model of source zone.

This study was performed as part of a larger research project termed CORONA (Consortium for Research on Natural Attenuation) to assess Monitored Natural Attenuation as a cost-effective scheme for remediation of upstream oil and gas (exploration and production) sites. The findings of this study are used in subsequent fate and transport modeling to develop a risk-based approach to predict Natural Attenuation variability at upstream oil and gas sites.

Hydrocarbon Impacted Site

The study site is a former flare pit site located in west-central Alberta, Canada. Solid stem augering was used for initial drilling. Soil logs showed heterogeneous distribution of clay, silt and sandy units (Armstrong, et al. 2004). The location of the former flare pit is roughly known to be in the north of the site. The exact limits, however, are not known. The site slopes from north to south. A few years ago, heavily contaminated soil at the north of the site was excavated to depths of 4 – 5 m and backfilled with clean soil. According to initial soil sampling analysis, free-phase hydrocarbons (NAPLs) were suspected to remain at the site. However, its presence had not been observed in the four nearest monitoring wells. The site was characterized through logging and sampling 16 boreholes drilled using the solid stem auger method to approximately 5 m below ground surface. Based on these data, 18 CPT-UVIF holes were advanced in two phases. The holes ranged in depth from 4 to 11 m below ground surface (Armstrong, et al. 2004). Figure 2 shows the locations of sampling points, monitoring wells as well as CPT-UVIF holes and geostatistical modeling domain. The modeling domain is 60 m in east-west direction, 80 m in north-south direction, and 16 m in depth.

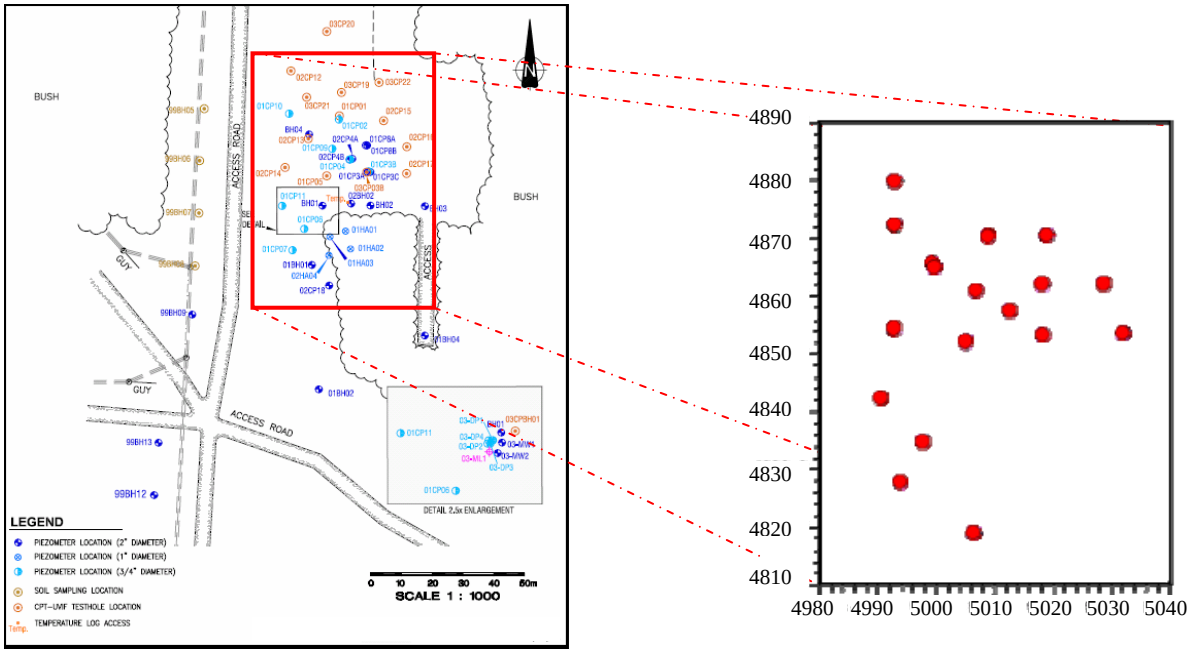

Figure 2: (left) locations of boreholes, monitoring wells and CPT-UVIF holes; and (right) Locations of 18 CPT-UVIF holes as well as domain for geostatistical study.

Geostatistical analysis for geological structure

The decision of which data should be pooled together for subsequent analysis is the "decision of stationarity" (Deutsch 2002). In other words, the decision of stationarity implies that mean (or prior probability) is independent from location (Goovaerts 1997). The decision of stationarity may be revised based on further steps of data analysis. For instance, while observing a bimodal (two peaks) histogram for data, one might want to consider separating the data into two classes with distinct statistical and geological properties (Deutsch 2002). In fact, separating the data set into more homogenous geologic and hydrogeologic zones improves the accuracy of the estimates. Indicator kriging offers an alternate method that is more appropriate for data showing non-stationarity in its basic statistics. Using indicator kriging to identify various 'soil types' or geological regions with distinct statistical and geological features enhances data homogeneity within sub-regions and makes the decision of stationarity more appropriate (Dagdelen and Turner 1996).

For every hole, the CPT-UVIF tool records tip resistance, sleeve friction, pore pressure and ultraviolet induced fluorescence at every 2.5 cm. Plotting cone resistance vs. friction ratio for every data location, one can observe distribution of data throughout the site and can identify different soil types. Using the plotted data (Figure 3) and the SBT chart (Figure 1), geological structure can be grouped into three sub-regions comprising soils with distinct statistical and hydrogeological features. Configuration of sampling points is clustered at the site which means all the data are not equally representative in summary statistics and must be weighted. Cell declustering is performed in this study using *declus* program in

GSLIB (Deutsch and Journel 1998). The resulted histogram of soil type data is displayed in Figure 3. According to Robertson (1998), each of these three soil types has an estimated range of hydraulic conductivities. Soil type one, with a frequency of 29.5 %, has hydraulic conductivity values approximately ranging from 1×10^{-11} m/s to 1×10^{-8} m/s. For soil type two, having a frequency of 55 % and covering majority of the site, hydraulic conductivity values approximately range from 1×10^{-9} m/s to 1×10^{-5} m/s. Soil type three, with a frequency of 15.5 %, has hydraulic conductivity values approximately ranging from 1×10^{-5} m/s to 1×10^{-2} m/s.

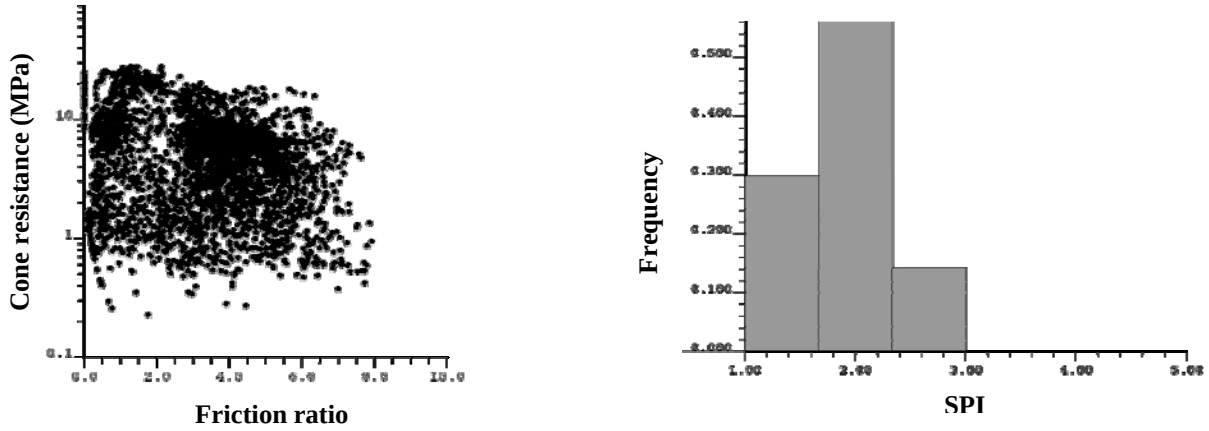

Figure 3: (left) Cone resistance vs. friction ratio values for 18 CPT cones; and (right) histogram of declustered soil type data.

Identifying directions of geological continuity

In presence of stratification and layering in geological structure, the decision of stationarity may no longer be appropriate. Even though all data have been already divided into three groups based on their statistical and geological features, it is still necessary to delineate the correct directions of geological continuity and detect any inclination in geological units. This requirement is a direct result of two important facts: (1) in geostatistical analysis the model is constructed on a Cartesian grid; and (2) the bounding surfaces between the layers correspond to a specific geologic time that separates two different periods of deposition or a period of erosion or consolidation followed by deposition, and are not often horizontal (Deutsch 2002). Thus, prior to calculation of directional variograms for different categories, a vertical coordinate transformation must be performed, considering various common deposition-erosion or consolidation-erosion scenarios.

As a standard practice, horizontal variograms are calculated after each coordinate transformation and the scenario showing highest degree of correlation is retained and the rest of the geostatistical modeling is done in the new coordinate system. The final results are ultimately back-transformed to original coordinate system. Four different deposition-erosion scenarios are schematically shown in Figure 4. For the present site, the original vertical coordinates happened to show highest degree of continuity (elevation scenario).

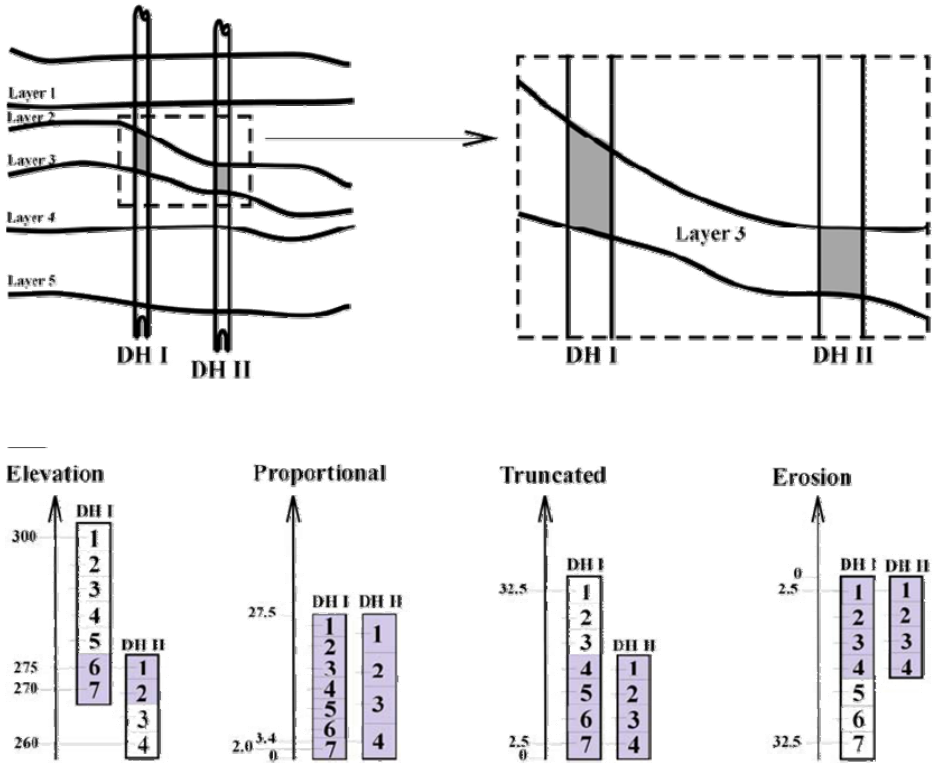

Figure 4: (top) A five-layer geological structure, samples taken from layer 3; and (bottom) Various coordinate transformation scenarios are calculated and shown. The shaded composites represent horizontal variogram calculation pairs (McLennan, 2004)

Modeling indicator variograms

Unlike Gaussian techniques, indicator formalism is capable of incorporating different spatial continuity for different categories. Indicator variograms are calculated for each category using the available site-specific data, using GSLIB (Deutsch and Journel 1998). The data used in calculation of indicator variograms are the data which have been transformed to soil type indices (1's, 2's and 3's for three different soil types). Figure 5 shows calculated and modeled variograms in horizontal and vertical directions for soil type 2. Similar directional variograms were calculated and modeled for soil types 1 and 3. The horizontal solid lines on the variograms show the sill, which represents maximum variability associated with each soil type in the modeling domain. It can be calculated by $p(1-p)$ where $p = F(z_k)$ is the global proportion of indicator variable before declustering. The range of a variogram is the horizontal distance between the origin of the variogram and the point at which variogram reaches to the sill. As the range becomes larger, smaller variability is observed in nearby data. Comparing the ranges of vertical and horizontal variograms in Figure 5, the effect of stratification can be clearly observed, since the vertical range is much smaller than the

horizontal range. It should be noted that spherical structure has been used in modeling variograms for all three soil types.

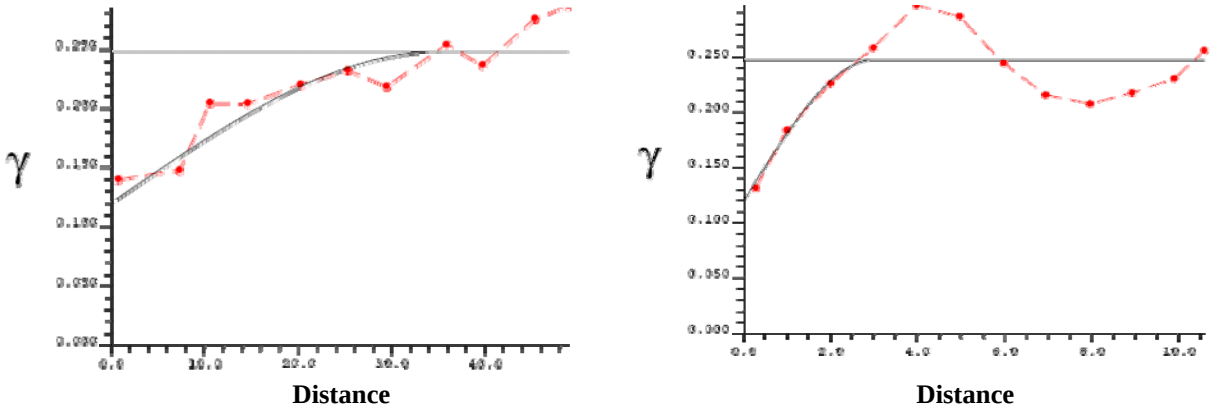

Figure 5: Horizontal variogram for soil type 2 (left) and Vertical variogram for soil type 2 (right); dashed lines and solid lines show calculated (experimental) and modeled variograms, respectively.

Indicator kriging and Sequential Indicator Simulation (SIS)

Indicator kriging (IK) (Deutsch and Journel 1998) and simulation are used to directly estimate the distribution of uncertainty in the categorical variables (i.e. soil types 1, 2, 3). As the first step in indicator formalism, site-specific data are coded as indicator values (Deutsch 2002), using:

$$i(\mathbf{u}_\alpha; z_k) = Prob\{\text{soil type } k \text{ being present}\} = \begin{cases} 1, & \text{if soil type } k \text{ is present at } \mathbf{u}_\alpha \\ 0, & \text{otherwise} \end{cases} \quad (1)$$

The stationarity prior probabilities of different soil types ($p(k),\ k=1,\ 2,\ 3$) have been determined using the histogram of declustered data (Figure 3). Based on figure 3, $p(1)=0.295$, $p(2)=0.55$, and $p(3)=0.155$. According to (1), residual data can be written as:

$$Y(\mathbf{u}_\alpha; z_k) = i(\mathbf{u}_\alpha; k) - p(k), \quad \alpha = 1, 2, \ldots, n, \quad k = 1, 2, 3 \quad (2)$$

According to Deutsch (2002), kriging of these residual data is used to derive the probability of occurrence of each soil type at every unsampled location. Thus, the model of uncertainty at every unsampled location **u** will be:

$$p_{IK}(\mathbf{u}; k) = \sum_{\alpha=1}^{n} \lambda_\alpha(k).[i(\mathbf{u}_\alpha; k) - p(k)] + p(k), \quad k = 1, 2, 3 \quad (3)$$

where the subscript *IK* denotes Indicator Kriging, λ_α's are weighting factors which account for closeness to data points as well as overall uncertainty in the domain and redundancy in nearby data. These weighting factors are calculated using the Simple Kriging (SK) system of equations. Variogram measures of correlation are used in constructing the SK system of equations.

The estimated probabilities must be non-negative and sum to one. As these requirements are not often fully satisfied by indicator kriging (IK) with categorical variables, a post-correction procedure is often performed.

Sequential Indicator Simulation (SIS) (Deutsch and Journel 1998) is a Monte Carlo simulation technique built on Indicator Kriging (IK) explained above. In order to populate the whole modeling domain with simulated values, grid nodes are visited sequentially in a random path. At each grid node the following procedure is repeated (Deutsch 2002): (1) searching for nearby data and previously simulated values, (2) performing IK to build a distribution of uncertainty, and (3) drawing a simulated value from the distribution of uncertainty.

Analyzing and post-processing of the results

As a result of Sequential Indicator Simulation, a large number of equi-probabale soil-type realizations are generated (Figure 6). These realizations reproduce the input data equally well. There are a number of checks which have been done to validate the model as a fairly good representative for the unknown reality: (1) reproduction of input statistics such as histogram and variograms, (2) honoring input data, (3) consistency with the available information about geology of the site, as well as checking the model predictions by (4) closeness of estimated probabilities to the true soil types (both for CPT data as well as borehole logs), and (5) accuracy of the local probabilities.

As observed in Figure 6, SIS realizations often show unrealistic short-scale variations. Using 'maximum a-posteriori selection' technique (MAPS), (Deutsch and Journel 1998), the realizations are cleaned from these short-scale variations and slight deviations from global proportions (order relations problem) are controlled and fixed.

The cleaned realizations are then used in (1) development of a 3D likelihood map for 'Soil Type' in the modeling domain, (2) stochastic simulation of hydraulic conductivity throughout the site, and (3) development of a prior probability map for NAPL contamination.

Figure 7 shows two cross-sectional views of the 3D likelihood map for soil type as well as CPT profile locations. The magnitude of cone resistance is shown on the cone profiles. As shown in the cross-sectional views, there is a large sandy layer (soil type 3) in depths from 1 m to 7 m extended to the northwest of the site. While, south of the site is mainly comprised of lower permeability units (soil types 1 and 2). Topography has been also displayed. The site generally slopes from the north to the south. The very high likelihood for the presence of a large sandy layer (at specific depths) on the northwest of the site should be considered in

design of any remediation scheme. The region south of the site (especially in shallower depths) is less likely to be a good pathway for contaminants to travel further downstream. Deeper areas on the south portion of the site, however, are more likely to be good pathways for transport of contaminants. It should be noted that based on independent site observations (borehole logs) the results of the model show the continuity and extent of geological features very well.

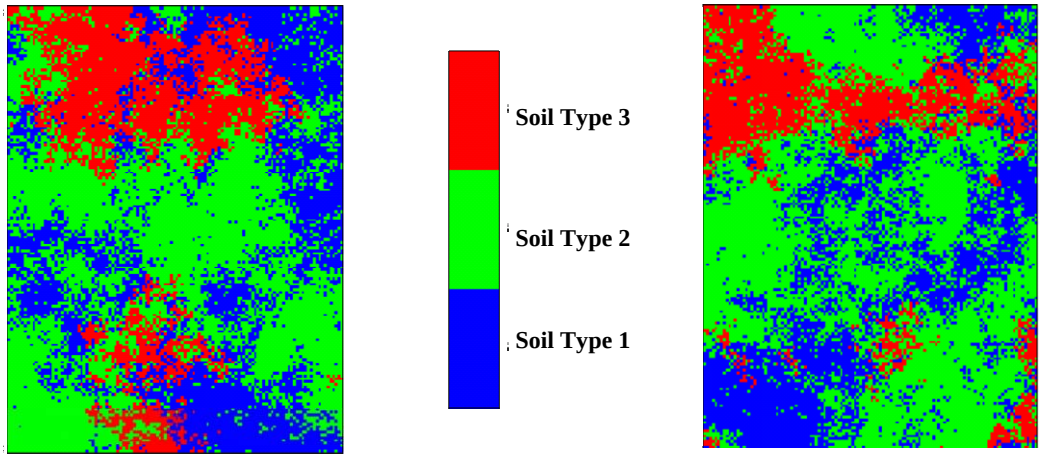

Figure 6: Planar views of two equi-probable realizations showing distribution of three soil types throughout the site. Theses realizations honor the input data (site-specific samples) and input statistics very well. The above slices are planar views taken at mid-height of the modeling domain.

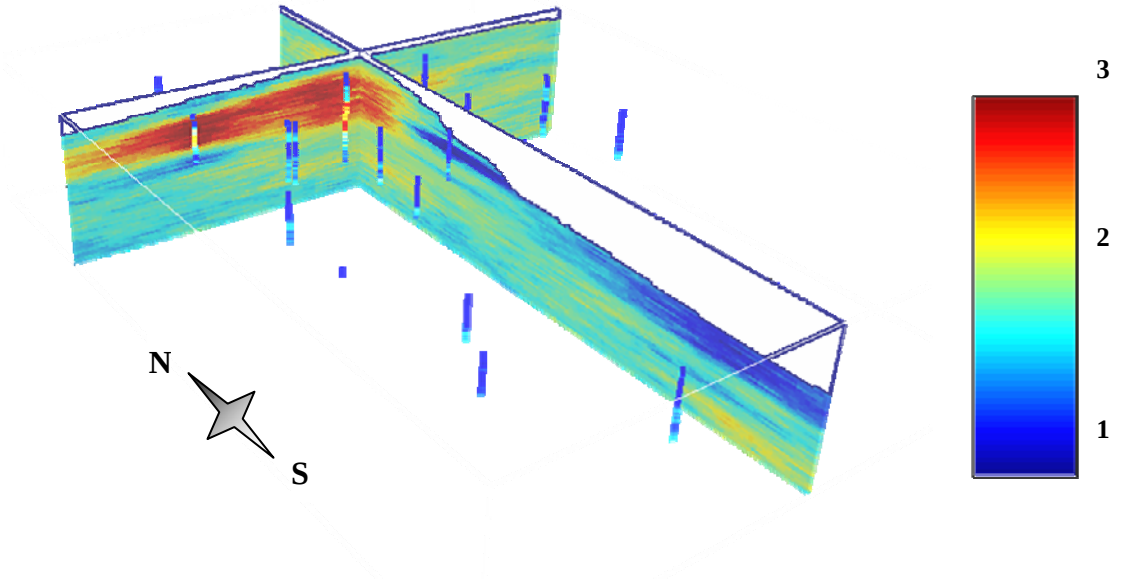

Figure 7: Two cross-sectional views of the 3D likelihood map for soil types. There is a large sandy layer (soil type 3) on northwest of the site. While, south of the site is mainly comprised of lower permeability units (soil types 1 and 2). Topography has been also displayed. The site generally slopes from the north to the south.

The generated soil-type realizations are also used to generate profiles of hydraulic conductivity for subsequent fate and transport modeling. When plotting histogram of sparse hydraulic conductivity data from the site, it is observed to be highly skewed and has a bi-modal shape. Assigning separate Gaussian distributions of hydraulic conductivity (with different means and variances) to each of the three soil types facilitates reproduction of the bi-modal shape for hydraulic conductivity distribution in every realization. These equi-probable realizations may then be used as input for stochastic (Monte Carlo) simulation of fate and transport for dissolved contaminants.

The soil-type realizations are also used in the development of a 3D prior probability map for presence of free-phase product (NAPL) at the site. Later in this paper, the correlation between soil type and NAPL presence is discussed and the prior probability map will be developed.

Geostatistical analysis for contaminant source zone

As stated before, UVIF data may be unrealistically affected by aggregate size. This introduces an artifact in distribution of free-phase product, if one directly relates UVIF data to NAPL concentrations. To avoid this artifact, a threshold value of UVIF voltage is introduced in this study and a model of presence/absence is developed for NAPL contamination. Results of this modeling effort introduce a risk-based framework for contamination.

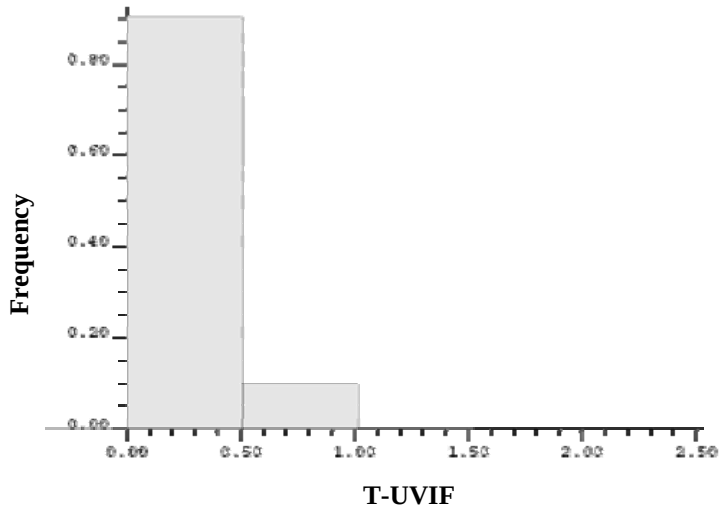

Figure 8: Histogram of declustered binary T-UVIF data for NAPL contamination

First, a model of contaminant source zone is developed solely based on available UVIF data. This model, however, does not show the lateral spread of contaminant plume appropriately. For the NAPL plume to conform to important geological features, the site-specific correlation between presence of NAPL and soil type is incorporated into the model

as secondary information. The results of this 'co-simulation' are then compared to those of the original model of contaminant source zone.

Modeling contaminant source zone using Truncated UVIF (T-UVIF) data

The UVIF output is recorded in volts. For this site, the minimum and maximum recorded values for UVIF output are 0.4 and 8.79 volts, respectively. After a series of sensitivity analyses, a threshold of 1.2 volts was selected to truncate the data and develop a binary absence/presence model. Selection of this threshold is an important step and it is still subject to further research.

Figure 8 provided the histogram of binary absence/presence data, showing that 10 percent of the data are identified as contaminated. Assuming stationarity in the data, this means 10 percent of the whole site is considered contaminated.

Figure 9 shows the directional indicator variograms for T-UVIF data. The ranges of variograms in binary models are related to the perimeter of the objects (or plumes in this study) in a 3D space (Monestiez, et al. 2001). This relationship may be used to obtain an estimate of average sizes of plumes.

Indicator kriging (IK) and sequential indicator simulation (SIS) are performed after variogram modeling. According to equation (3), IK gives an estimate of local uncertainty at every location. GSLIB (Deutsch and Journel 1998) was used to perform IK and SIS. SIS procedure for modeling the source zone is the same as procedure for the model of soil types presented above.

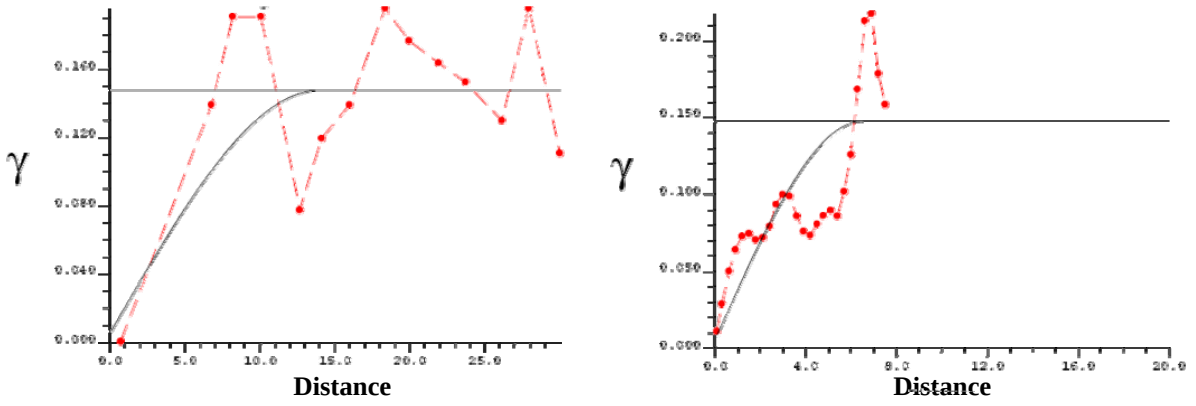

Figure 9: Horizontal variogram (left) and vertical variogram (right) for model of contamination; dashed lines and solid lines show experimental and modeled variograms, respectively.

A large number of equi-probable realizations are generated. These realizations are used in the development of a 3D probability map for contamination. Defining a series of probability thresholds, the probability map can be visualized in a risk-based format. Figure 10 shows planar views of a series of 3D risk maps. Each of these risk maps shows the extent of the NAPL plume for a certain degree of associated risk. For instance, for the map with an

associated risk of 90 percent (Figure 10a), there is a 90 percent or more probability for the soil in the marked areas to be contaminated. Figure 11 shows the lateral and vertical extent of the NAPL plume with an associated risk of 30 percent or more. Figure 11 shows that the plume seems to have a bulky shape and does not follow stratification patterns observed in soil structure (Figure 7). Based on this, it is desirable to somehow incorporate the model of geological continuity and soil structure into the model of NAPL plume. As observed later in this study, if stratification is not taken into account, the plume will be unrealistically small and bulky.

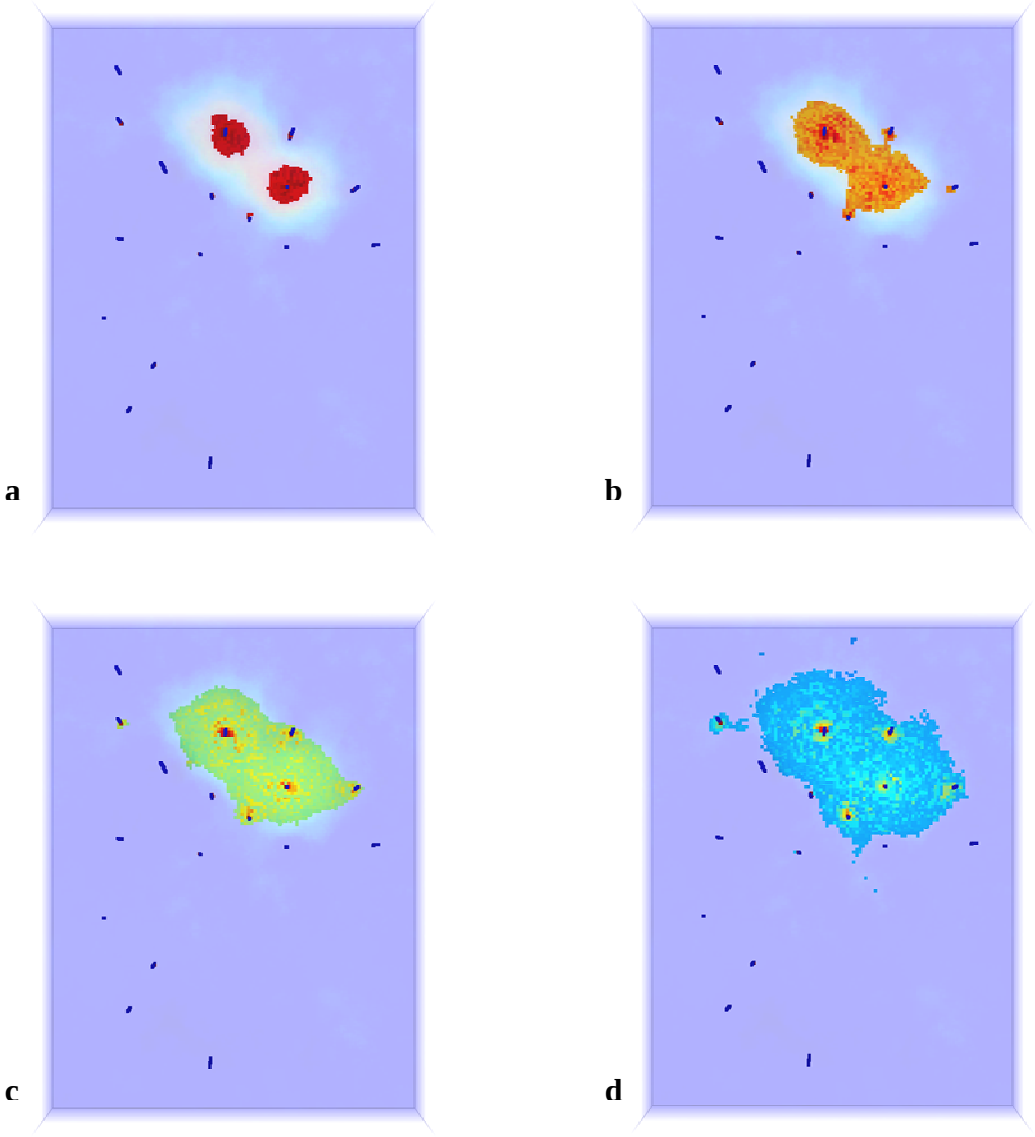

Figure 10: Planar views of risk maps showing extent of NAPL plume for different levels of risk: (a) 90 percent, (b) 70 percent, (c) 50 percent, and (d) 30 percent.

Modeling contaminant source zone using T-UVIF data and model of geological structure as secondary information

The model of geological structure can be successfully used as secondary information to improve the model of the contamination source zone. There are a number of reasons for this:

1. There is an evident correlation between presence of free phase product (NAPL) and grain size of aggregates: The larger the grain sizes and pore spaces, the more likely presence of free phase product;
2. More information is often available about geological structure from site investigations. Moreover, obtaining information about geology of the site is often much cheaper, easier and more reliable as compared to gathering information about contaminant distribution;
3. Unlike contaminant distribution, geological structure often shows higher ranges of correlation and larger distances of continuity. This can be observed in Figures 5 and 9. In fact, direction of continuity and inclination of strata play important roles in prediction of NAPL distribution in the subsurface.

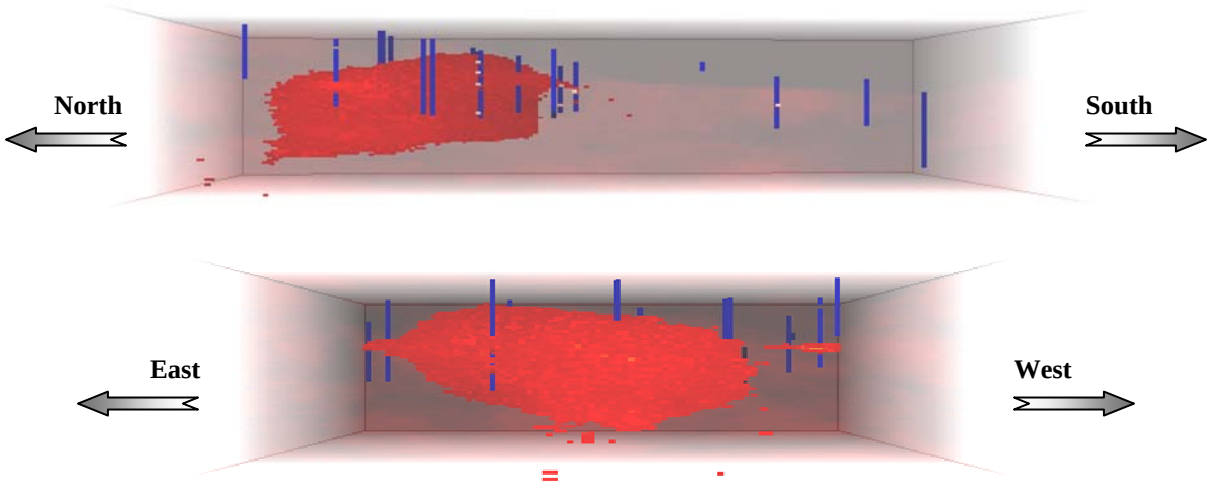

Figure 11: Cross-sectional views of risk maps showing vertical and lateral extent of NAPL plume for a risk of 30 percent.

To incorporate the geological model in the model of the source zone as secondary information, first of all correlation between site-specific soil type data and T-UVIF data must be determined. Table 1 shows this correlation. According to the table, whenever soil type 3 is observed at a location, there is a probability of 14.67 percent for that location to be contaminated. This probability is 8.95 for soil type 2 and 8.68 for soil type 1. The cokriging estimate is expressed as;

$$\hat{i}(\mathbf{u};k)=\sum_{\alpha=1}^{n}\lambda_\alpha\cdot i(\mathbf{u}_\alpha;k)+\left[1-\sum_{\alpha=1}^{n}\lambda_\alpha\right]\cdot p(k|ai(\mathbf{u})) \qquad (4)$$

in which, $\hat{i}(\mathbf{u}_\alpha;k)$ is the probability of presence of NAPL at location **u**, $i(\mathbf{u}_\alpha;k)$ is the indicator data for the presence or absence of NAPL (a binary variable) and is defined in a way similar to equation (1), λ_α's are weighting factors which account for closeness to data points as well as overall uncertainty in the domain and redundancy in nearby data. The term $p(k|ai(\mathbf{u}))$ represents prior probability for presence of NAPL. This is a location-dependent attribute and is calculated by assigning the correlation factors summarized in Table 1 to a large number of equi-probable soil-type realizations (Figure 6). According to equation (4), for every location of the modeling domain $p(k|ai(\mathbf{u}))$ receives a higher weight, if there are smaller number of data in close proximity of location being estimated and vice versa.

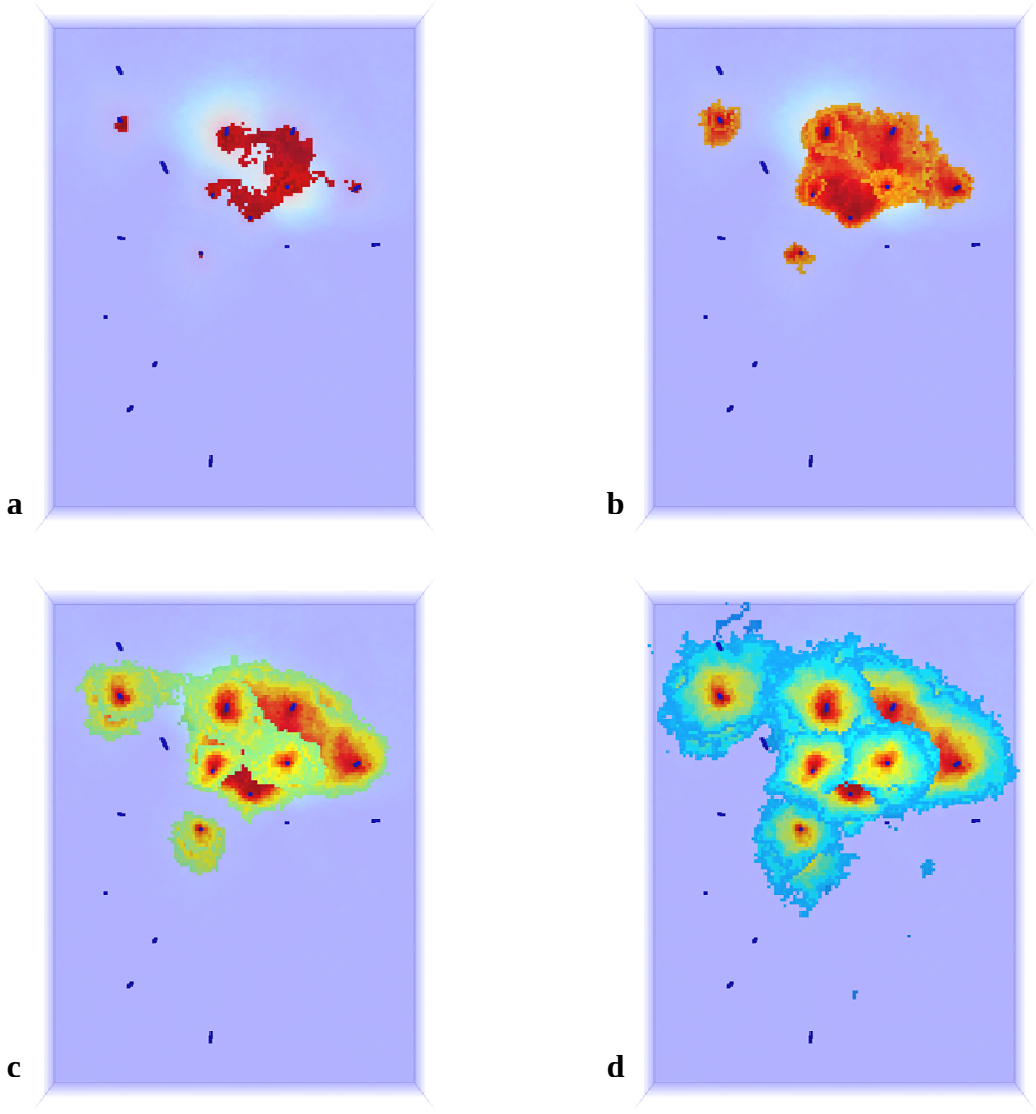

Figure 12: Planar views of risk maps showing extent of NAPL plume, resulted from **cosimulation** for different levels of risk: (a) 90 percent, (b) 70 percent, (c) 50 percent, and (d) 30 percent.

	Presence (%)	*Absence (%)*
Soil Type 1	**8.68**	**91.32**
Soil Type 2	**8.95**	**91.05**
Soil Type 3	**14.67**	**85.33**
Weighted Average	**10**	**90**

Table 1: Correlation factors between soil type data and presence of contamination

The results of the co-simulation are shown in Figures 12 and 13. Comparing Figure 13 to Figure 11, one can evidently observe the capability of the co-simulation in modeling lateral continuity of NAPL plumes. Also, comparing Figure 12 to Figure 10 shows that if the geological continuity is not incorporated into the model of source zone, size and lateral extent of the plume may be significantly under-estimated.

The risk maps, developed for contaminant source zone, clearly show the extent of contamination for different risk levels. These are valuable tools for sample optimization purposes, whenever additional sampling is required. Including other controlling factors, such as groundwater fluctuations, as secondary variables can also enhance the model's prediction capability. The risk maps and likelihood maps can also be used in conjunction with other design factors to increase the effectiveness of active remediation schemes to reduce the overall cost of remediation projects.

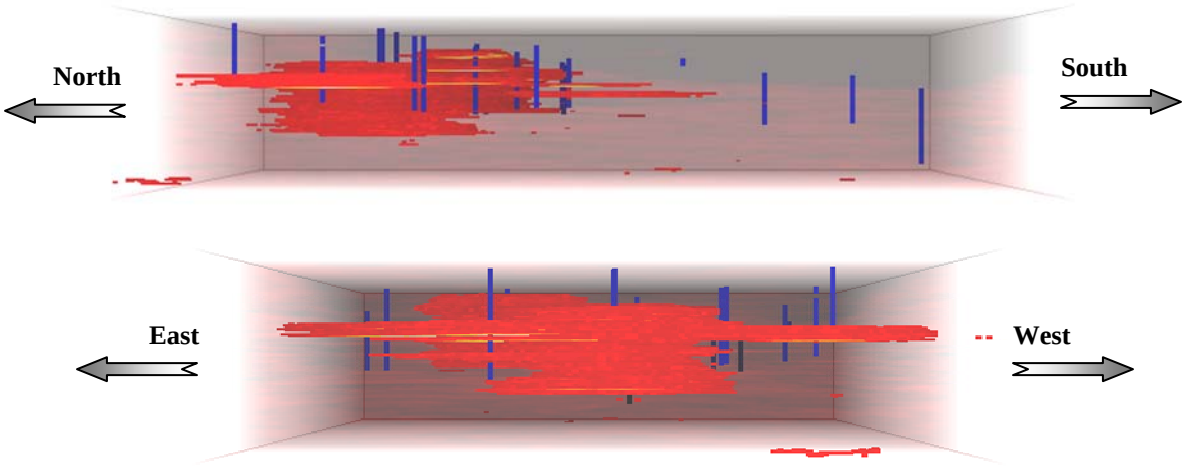

Figure 13: Cross-sectional views of risk maps, resulted from **cosimulation**, showing vertical and lateral extent of NAPL plume for a risk of 30 percent.

Conclusions

Geostatistical Modeling is a powerful tool to study geological structure by providing information about continuity of subsurface strata and location of high permeability conduits. It is also applicable in the reproduction of representative hydraulic conductivity values throughout the site.

Geostatistical analysis can be used to delineate contaminant source zone and gives an estimate of plume size. The model of contaminant source zone can be successfully improved by incorporating some secondary information such as geological structure. This secondary information can be any property which is some how quantifiable. Indicating directions of maximum likelihood for contamination and lateral and vertical extent of NAPL plume, the model can be used in sampling optimization programs.

Acknowledgments

The first author would like to acknowledge WorleyParsons Komex and in particular Mr. Morris Maccagno and Mr. Craig Campbell for their constructive comments and support throughout this research work.

References

Armstrong, J. E., C. V. Deutsch, and K. W. Biggar, 2003: *Geostatistical Assessment of Cone Penetrometer Test Data for Contaminant Assessment Based on Ultraviolet Induced Fluorescence*. Proceeding of the 56th Canadian Geotechnical Conference and the 4th Joint CGS/IAH-CNC Groundwater Specialty Conference, Winnipeg, MB, Canada, September 29-October 1. 17 pp.

Canadian Council of Ministers of the Environment, 2001: Reference Method for the Canada-Wide Standard for Petroleum Hydrocarbons in Soil - Tier1 Method. , 44 pp.

Dagdelen, K., and K., Turner, 1996: *Importance of Stationarity of Geostatistical Assessment of Environmental Contamination*. Geostatistics for environmental and geotechnical applications. Vol. 1283. ASTM, 280 pp.

Deutsch, C. V., 2002: *Geostatistical Reservoir Modeling.* Oxford University Press. 376 pp.

Deutsch, C. V. and A. G. Journel, 1998: GSLIB : geostatistical software library and user's guide. 369 pp.

Goovaerts, P., 1997: *Geostatistics for natural resources evaluation.* Oxford University Press, 483 pp.

Kram, M. L., A. A. Keller, S. M. Massick, and L. E. Laverman, 2004: Complex NAPL site characterization using fluorescence Part 1: Selection of excitation wavelength based on NAPL composition. *Soil and Sediment Contamination*, 13, 103-118.

Lunne, T., P. K. Robertson, and J. Powell, 1997: *Cone Penetration Testing in Geotechnical Practice.* Thomson Professional Publishers. 305 pp.

McLennan, J. A., 2004: *Using the Variogram to establish the stratigraphic correlation structure*. Sixth Annual Report of the Centre for Computational Geostatistics, University of Alberta, Canada, 405 pp.

Monestiez, P., D. Allard, and R. Froidevaux, 2001: *Average length of objects defined from binary realizations: effects of Discretization and covariance parameters.* GeoENV III: geostatistics for environmental applications: proceedings of the third European Conference on Geostatistics for Environmental Applications held in Avignon, France, November 22-24, 2000. Kluwer Academic, 323 - 333.

Robertson, P. K., 1998: Applications Guide - CPT. Geotechnical Center, University of Alberta, Canada. 67 pp.

Robertson, P. K., R. G. Campanella, D. Gillespie, and J. Greig, 1986: *Use of piezometer cone data*. Proceedings of the ASCE Specialty Conference: In Situ '86. ASCE (Geotechnical Special Publication 6), New York, NY, USA, 1263-1280.